# Effects of Ca substitution and the pseudogap on the magnetic properties of $Y_{1-x}Ca_xBa_2Cu_3O_{7-\delta}$

S. H. Naqib,[1,2,*] J. R. Cooper,[1] and J. W. Loram[1]

[1]*Department of Physics, University of Cambridge, J. J. Thomson Avenue, Cambridge CB3 OHE, United Kingdom*

[2]*Department of Physics, University of Rajshahi, Raj-6205, Bangladesh*

(Received 17 August 2007; revised manuscript received 16 December 2008; published 26 March 2009)

The effects of planar hole content, $p$, on the static magnetic susceptibility, $\chi(T)$, of $Y_{1-x}Ca_xBa_2Cu_3O_{7-\delta}$ polycrystalline samples were investigated over a wide range of Ca($x$) and oxygen contents. We have again found that the pseudogap in the quasiparticle spectral weight appears abruptly below a planar hole content $p = 0.190 \pm 0.005$. After considering possible effects of magnetic impurity phases, we conclude that nonmagnetic $Ca^{2+}$, in the $3p^6$ state, induces a Curie-like contribution to $\chi(T)$ that increases systematically and nonlinearly with $x$ but is almost independent of $p$. We argue that this arises from statistical clusters containing two or more nearest-neighbor Ca atoms.

DOI: 10.1103/PhysRevB.79.104519 PACS number(s): 74.72.Bk, 74.25.Ha, 74.25.Dw, 74.62.Dh

## I. INTRODUCTION

The properties of high-$T_c$ copper oxide superconductors (HTS) in the normal and the superconducting (SC) states are highly dependent on the number of doped carriers per copper oxide plane, $p$, and one of the most widely studied phenomena is the so-called normal-state pseudogap (PG).[1–4] Effects of the pseudogap are observed in the $T$-$p$ phase diagram of the cuprates over a certain doping range, extending from the underdoped (UD) to slightly overdoped (OD) regions. Many of the unusual properties can be interpreted in terms of a reduction in the quasiparticle (QP) density of states (DOS) near the chemical potential.[1–6] At present the experimental and the theoretical situations regarding the origin of the pseudogap are rather inconclusive.[2,4]

Here we report a systematic study of the static magnetic susceptibility, $\chi(T)$, of polycrystalline $Y_{1-x}Ca_xBa_2Cu_3O_{7-\delta}$ (Ca-Y123) over a wide range of $p$ as well as further heat-capacity results for a representative sample. One advantage of Ca($x$) substitution is that the overdoped region can be studied, up to $p \sim 0.23$ with $x = 0.20$.[7,8] To our knowledge, detailed $\chi(T)$ measurements of Ca-substituted Y123 have not been reported so far. Based on experimental evidence[1,3,5] that $\chi(T)$ and $S/T$, where $S$ is the electronic entropy, show similar behavior, analysis of $\chi(T,p)$ data gives important information about the $T$ and $p$ dependences of the low-energy electronic density of states for this representative hole-doped cuprate. The variation in the DOS, $N(\varepsilon)$ with energy $\varepsilon$ is at the heart of any problem associated with the pseudogap so $\chi(T,p)$ is a simple but powerful way of studying this quantity. The intrinsic spin part of $\chi(T,p)$, the static susceptibility, $\chi_{spin}$ is a measure of the QP spectral density near the Fermi level. For Fermi liquids and in the absence of exchange enhancement, it can be expressed as

$$\chi_{spin}(T) = \mu_B^2 \langle N(\varepsilon)\rangle_T, \quad (1)$$

where $\langle N(\varepsilon)\rangle_T \equiv \int N(\varepsilon)(\partial f/\partial\varepsilon)d\varepsilon$, is the thermal average of the DOS, $\mu_B$ is the Bohr magneton, and $f$ is the Fermi function. Therefore, $\chi_{spin}$ at any particular temperature, $T$, represents the average of $N(\varepsilon)$ over an energy region $\sim\varepsilon_F \pm 2k_BT$.[5]

The main observations from the present study are: (i) we again find that the PG appears abruptly for compounds with $p < 0.19$. (ii) Nonmagnetic Ca substitution induces a Curie term in $\chi(T)$ that is independent of the value of $p$. (iii) We argue that this Ca-induced Curie term is caused by clusters of two or more nearest-neighbor $Ca^{2+}$ ions. If this is true, it has implications for establishing the number of mobile holes, $p$, in materials such as LSCO and Bi:2201, where the hole content is varied systematically by doping with a relatively large number of altervalent atoms.

## II. EXPERIMENTAL DETAILS

Polycrystalline samples of $Y_{1-x}Ca_xBa_2Cu_3O_{7-\delta}$ were synthesized by standard solid-state reaction methods from high-purity powders. Details of sample preparation and characterization can be found in Refs. 9–11. A single sample was often used for each Ca content, the oxygen deficiency, $\delta$ and hence $p$ was varied by annealing at fixed temperatures and oxygen partial pressures and quenching the sample into liquid nitrogen.[10] Most normal and SC state properties including $E_g$ (the characteristic PG energy scale) of HTS are strongly dependent on $p$, which should therefore be determined as accurately as possible. We have used the room-temperature thermopower, $S[290\text{ K}]$,[12,13] as well as the parabolic $T_c$-$p$ (Ref. 14) relation to determine $p$ for all samples. These two methods gave almost identical values of $p$. We measured $T_c$ using both resistivity and low-field ac susceptibility with an alternating field $H_{rms} = 0.1$ Oe, and frequency $f = 333.3$ Hz.[13] $T_c$ values obtained with these two methods agree to within 1 K for all the samples. Electron probe microanalysis (EPMA) was performed to verify the chemical composition and homogeneity of all samples.

Quantum Design MPMS2 and MPMS XL superconducting quantum interference device (SQUID) magnetometers were used for the magnetic measurements reported here, for data from 5–400 K and 5–330 K, respectively. A magnetic field of 5 T was applied, with field-linearity checks at 300 and 100 K, and the background signal from the sample holder was measured and subtracted from the raw data. Measurements of the first 20% Ca sample (Ca20 I) were made at the same time as the original heat-capacity work[5] on samples

 

TABLE I. Parameters for well-oxygenated samples including values of $\chi_0$ and $C_{tot}$ from high-$T$($HT$) fits to $\chi(T)=\chi_0+C_{tot}/T+\beta/T^2$ from 125–330 or 400 K. Also shown are the contributions ($C_{ESR}$) to the Curie constant arising from unwanted paramagnetic phases detected by ESR. The $^*$ symbol shows samples for which there was a ferromagnetic background at the time of the ESR measurements, giving larger uncertainty in $C_{ESR}$. The $^{**}$ symbol shows impurity term estimated from heat-capacity data for sample III. $C_{corr}=C_{tot}-C_{ESR}$ except for the 0% Ca sample where the unphysical negative value of $C_{tot}$ arises from the PG, and therefore $C_{corr}=0$.

| Sample (Ca%) | EPMA [$x$(Ca)] | $p$ (holes/Cu) | $\chi_0$ (HT fit) ($10^{-4}$ emu/mol) | $C_{tot}$ ($10^{-4}$ emu K/mol) | $C_{ESR}$ ($10^{-4}$ emu K/mol) | $C_{corr}$ ($10^{-4}$ emu K/mol) |
|---|---|---|---|---|---|---|
| 0 | | 0.176 | 2.78 | −30.8 | | 0 |
| 5 | $0.049\pm0.006$ | 0.203 | 2.88 | 50 | $34^*$ | 16 |
| 10 | $0.105\pm0.010$ | 0.210 | 2.50 | 237 | $34\pm4$ | 203 |
| 20 I | $0.195\pm0.012$ | 0.220 | 2.85 | 370 | $30^*$ | 340 |
| 20 II | $0.20\pm0.03$ | 0.215 | 2.46 | 481 | $82\pm11$ | 399 |
| 20 III | | 0.218 | 2.61 | 496 | $157\pm26^{**}$ | 339 |

from the same preparation batch (I). Powder x-ray diffraction (XRD) patterns of all the samples studied here showed phase purity to within 1%. Raman spectroscopy studies suggested that the dominant magnetic impurity is $BaCuO_{2+z}$ because a peak at $\sim$640 cm$^{-1}$ (Ref. 15) with variable intensity was observed for different Ca-Y123 samples. Batch II of the 20% Ca-Y123 compound (Ca20 II) had a higher intensity peak than batch I and the compounds with lower Ca content, in qualitative agreement with the electron-spin-resonance (ESR) results described below.

Room-temperature ESR at 9 GHz was used to search for unwanted magnetic impurity phases. Two lines in the derivative spectra with peak to peak widths $\sim$200 and $\sim$1000 Gauss were usually visible, the ESR intensity generally being dominated by the broader line. Double integration of the ESR spectra and calibration with a known mass of a standard sample, pure $Y_2BaCuO_5$, gave values of the Curie constant ($C_{ESR}$) listed in Table I. Although the ESR data showed that 0.3–1% of the total number of Cu atoms were contained in impurity phases, *a-priori* there is some uncertainty[16–18] as to whether the broader line does indeed arise from $BaCuO_2$. Furthermore, because of the complex crystallographic and magnetic structure of $BaCuO_2$,[16,17] it is not clear that all Cu spins would be detected by room-temperature ESR. Later ESR experiments at lower $T$ (and in fact two of the room-temperature measurements shown in Table I) were hampered by the partial decomposition of the powder samples, giving a ferromagnetic component that was also seen in later SQUID magnetometer data but absent in the earlier SQUID data. Finally, partly as an extra check for magnetic impurity phases, the heat capacity, $C_v$, of a third highly overdoped 20%Ca-Y123 sample (Ca20 III), with $S$[290 K] $=-6$ $\mu$V/K giving $p=0.218$, was measured. This sample had a larger susceptibility than the two samples studied in detail, e.g., at 300 K $\chi T=0.143$ emu K/mole, but after correction for magnetic impurities detected via the heat capacity, $\chi(T)$ is reasonably consistent with data for the other two 20% Ca samples.

Figures 1 and 2 show plots of $\chi(T)$ and $\chi(T)T$ for the $Y_{1-x}Ca_xBa_2Cu_3O_{7-\delta}$ compounds at various values of $p$ and readily illustrate two important points. The first one, related to the existence of the pseudogap (discussed in the next section), is that both $\chi(T)$ and $\chi(T)T$ become strongly $p$ dependent

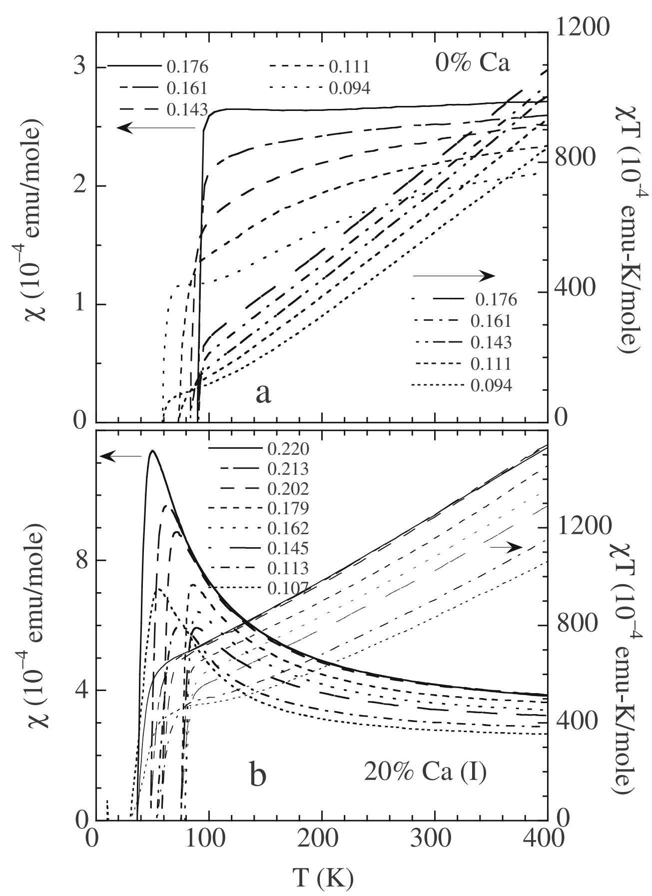


FIG. 1. $\chi(T)$ and $\chi(T)T$ for (a) $YBa_2Cu_3O_{7-\delta}$, and (b) $Y_{0.80}Ca_{0.20}Ba_2Cu_3O_{7-\delta}$ (first batch). $p$ values are shown and are accurate to $\pm0.004$.

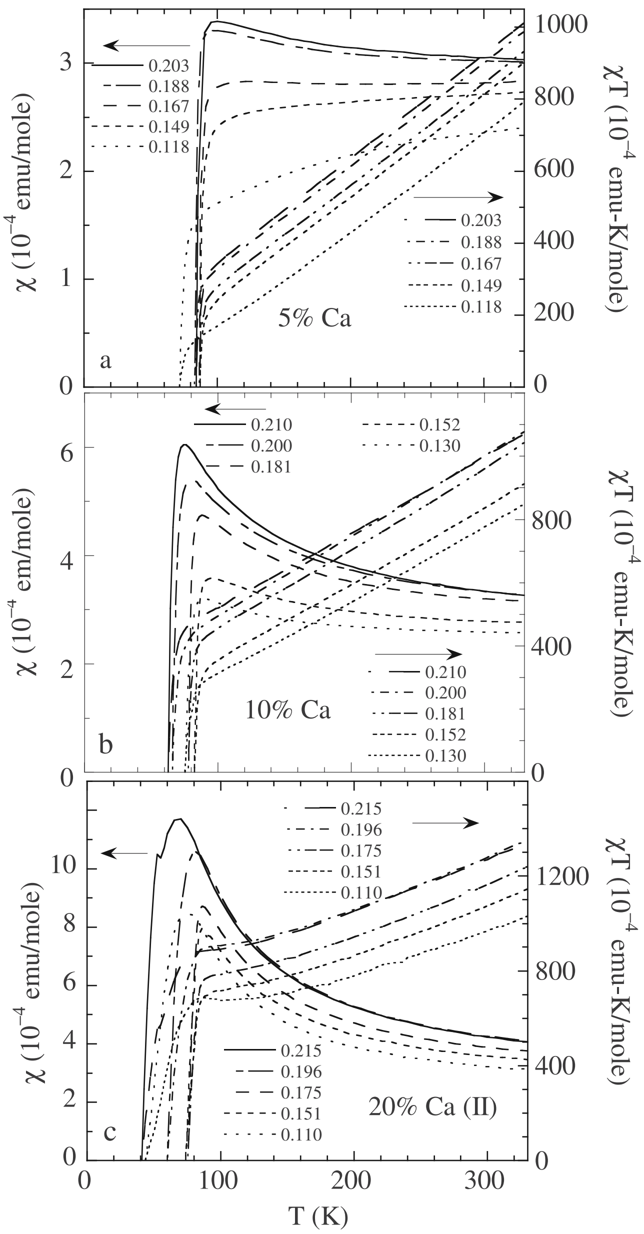


FIG. 2. $\chi(T)$ and $\chi(T)T$ for (a) $Y_{0.95}Ca_{0.05}Ba_2Cu_3O_{7-\delta}$, (b) $Y_{0.90}Ca_{0.10}Ba_2Cu_3O_{7-\delta}$, and (c)$Y_{0.80}Ca_{0.20}Ba_2Cu_3O_{7-\delta}$ (second batch). $p$-values are shown and are accurate to $\pm 0.004$.

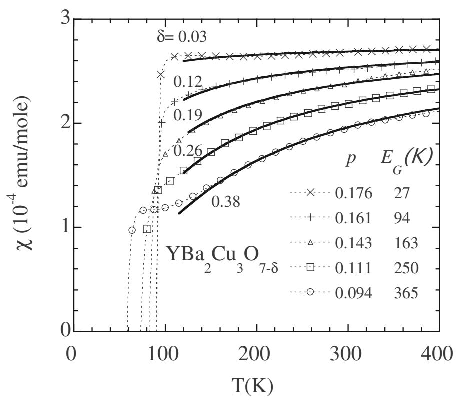


FIG. 3. Fits (full lines) of normal-state $\chi(T,p)$ data (Ref. 3) for polycrystalline $YBa_2Cu_3O_{7-\delta}$, with the oxygen deficiencies $\delta$ shown, to Eqs. (1) and (2) in text. The parameter $N_0$ was fixed at a value corresponding to $\chi = 2.75 \times 10^{-4}$ emu/mole for $E_g = 0$. Values of $E_g$ obtained from the fits are given in the figure.

dent *only* for $p < 0.19(\pm 0.005)$. The second important finding is that there is a systematic growth of Curie-like behavior in $\chi(T)$ with increasing Ca content. $\chi(T)$ for Ca-substituted Y123 shows features similar to Co- or Ni-substituted Y123.[6] This is quite surprising because unlike Co and Ni, Ca is nonmagnetic having a full outer shell, $3p^6$, in the doubly ionized state. Therefore, no Curie-like contribution to the magnetization is expected. It has been suggested that oxygen vacancies are induced in the $CuO_2$ planes by increasing levels of Ca substitution.[19] Electron irradiation studies[20] suggest that, if present, these vacancies would be strong perturbations similar to Zn/Cu substitution. We feel that in-plane oxygen defects are probably not important here because, in contrast to the effect of strong in-plane scattering by Zn atoms, $T_{cmax}$ (maximum $T_c$) and the Hall angle[21–23] are not altered very much by Ca substitution.

## III. DATA ANALYSIS

### A. Effect of the PG and Ca on the magnetic susceptibility

As mentioned in Sec. I, the striking correspondence between the spin susceptibility and the electronic entropy, $S$, or more precisely $S/T$, is well documented.[1,5,6] This suggests that we may interpret our $\chi(T,p)$ data in terms of the DOS for the cuprates, in spite of the presence of strong electronic correlations in these compounds. The electronic entropy has a simple physical meaning, $S(T)/k_B$ counts the total number of thermally excited charge and spin excitations in the electronic spectrum in an energy window a few $k_BT$ wide, centered on the chemical potential. The quantity $\chi_{spin}T$ on the other hand provides complementary information for the spin spectrum. Specifically, $k_B\chi_{spin}T = \langle\mu_z^2\rangle$, where $\langle\mu_z^2\rangle$ is the mean squared moment, and therefore $(k_B\chi_{spin}T)/\mu_B^2$ is a measure of the number of thermal spin excitations inside a similar energy window around the Fermi energy.[5,6] For a V-shaped gap in the DOS, namely, $N(\varepsilon) = N_0$ for $|\varepsilon - \varepsilon_F| > k_BE_g$ (where $E_g$ is the pseudogap energy scale expressed in degrees K) and $N(\varepsilon) = N_0|\varepsilon - \varepsilon_F|/k_BE_g$ for $|\varepsilon - \varepsilon_F| < k_BE_g$, $\chi_{spin}$ is given by Eq. (1) with[5,24]

$$\langle N(\varepsilon)_T\rangle = N_0[1 - D^{-1}\ln\{\cosh(D)\}], \tag{2}$$

where $D = E_g/2T$. Figure 3 shows fits of $\chi(T,p)$ data[3] for pure Y123 samples to Eqs. (1) and (2), with a $p$-independent value of $N_0$, from 400 K to $\sim T_c + 30$ K (to avoid significant SC fluctuations near $T_c$). $E_g(p)$ values obtained from the fits are shown in Fig. 3 and also plotted later in Fig. 6. Note that in Ref. 6 the measured $\chi(T,p)$ data were increased by $+0.4 \times 10^{-4}$ emu/mole corresponding to the zero of the spin susceptibility determined by nuclear magnetic resonance (NMR). In the present paper we have analyzed the measured data for all samples without making any offsets.

High-$T$($HT$) fits of $\chi(T)$ to a second-order polynomial, $\chi_0 + C_{tot}/T + \beta/T^2$, were made from 125 to 330 or 400 K.

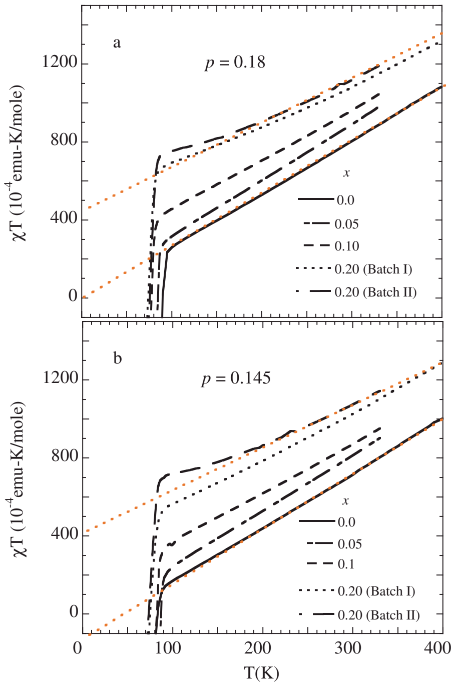


FIG. 4. (Color online) (a) $\chi(T)T$ for $Y_{1-x}Ca_xBa_2Cu_3O_{7-\delta}$ with $p=0.180\pm0.005$ and (b) $Y_{1-x}Ca_xBa_2Cu_3O_{7-\delta}$ with $p=0.145\pm0.005$. Ca contents ($x$) are shown in the figure. Dotted (red) lines show the high-$T$ fits with intercepts $C_{tot}$ at $T=0$ K.

Here $\chi_0$ is the $HT$ limit of $\chi_{spin}$ and $C_{tot}$ is the Curie constant including contributions both from Ca and possible magnetic impurity phases while $\beta$ allows for a range of nonzero Curie-Weiss temperatures $\theta$. Table I shows values of $\chi_0$ and $C_{tot}$ obtained from these $HT$ fits for well-oxygenated OD samples. For the 10 and 20% Ca-Y123 samples the values of $C_{tot}$ are much larger than those determined by ESR, $C_{ESR}$. This leads us to the surprising conclusion, justified in more detail in Sec. IV, that Ca substitution gives rise to a substantial Curie term.

$C_{tot}$ can also be found by linear extrapolation of $\chi T$ plots to $T=0$. However a nonzero value of $E_g$ gives a negative contribution to the $T=0$ intercept.[24] So therefore we should focus on the *changes* in the intercept ($C_{tot}$) with Ca content $x$ for a fixed value of $p$. The $\chi T$ plots in Figs. 1, 2, and 4 reveal that the changes in intercept with $x$ are essentially $p$ independent and therefore finite chain segments caused by oxygen deficiency cannot be making a significant contribution to $C_{tot}$. More generally they show that the changes in $\chi(T)T$ data for the same sample with different values of $p$ arise from changes in intrinsic spin susceptibility, $\chi_{spin}(T)$, in Eq. (1), with $p$. These differences, $\Delta\chi T$, show how the number of QP excitations inside an energy window of width $\sim\varepsilon_F\pm2k_BT$ changes with $p$. We have gathered other evidence from our earlier charge transport studies on $Y_{1-x}Ca_xBa_2Cu_3O_{7-\delta}$ (Refs. 4, 5, 10, 13, and 24) that a PG does not exist for $p>0.19\pm0.005$. It is therefore convenient to use $\chi(T)T$ for the largest value of $p$ ($>0.19$) as a reference. One major advantage of using $\Delta\chi T(p)=\chi T(p)-\chi T(p>0.19)$ is that it excludes $p$-independent contributions to $\chi(T)$, and therefore practically eliminates the terms that are not related to the QP DOS.

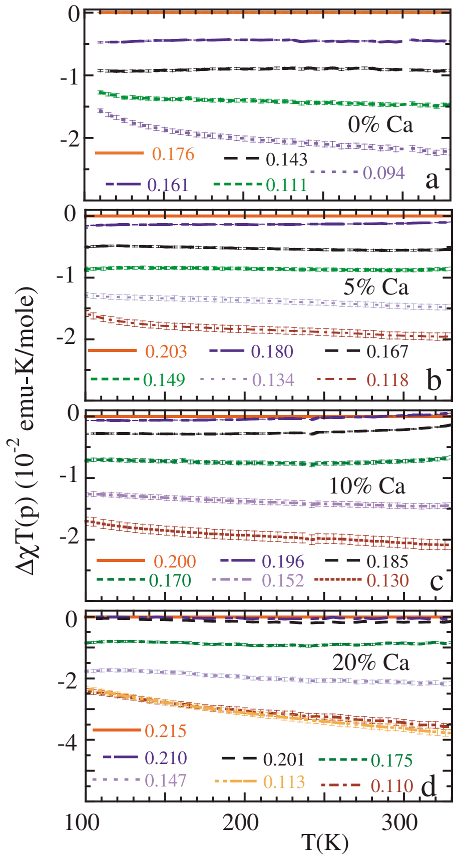


FIG. 5. (Color online) $\Delta\chi T(p)[\equiv\chi T(p)-\chi T(p_{ref})]$ for (a) pure Y123, $p_{ref}=0.176$. (b) $Y_{0.95}Ca_{0.05}Ba_2Cu_3O_{7-\delta}$, $p_{ref}=0.203$, (c) $Y_{0.90}Ca_{0.10}Ba_2Cu_3O_{7-\delta}$, $p_{ref}=0.201$, (d) $Y_{0.80}Ca_{0.20}Ba_2Cu_3O_{7-\delta}$, $p_{ref}=0.215$ (second batch) with one data set at $p=0.113$ for the first batch with $p_{ref}=0.220$. $p$-values are accurate to $\pm0.004$.

$\Delta\chi T(p)$ values for the $Y_{1-x}Ca_xBa_2Cu_3O_{7-\delta}$ compounds are shown in Fig. 5 in the temperature range from 100 to 330 K. Again the lower temperature limit is set above the region where significant superconducting fluctuations are present. Figure 5 highlights a number of interesting and important features, namely, (i) the sudden appearance of the pseudogap at $p\sim0.19$ and its growth with further underdoping manifested by the decrease in $\Delta\chi T(p)$ with decreasing $p$. This clearly illustrates the loss of QP states near the Fermi level. (ii) $\Delta\chi T(p)$ is close to zero for $p>0.19$, confirming the absence of a pseudogap for these hole contents. (iii) For values of $p$ that are not too low, a nonzero value of $E_g$ simply gives a constant downward shift in $\Delta\chi T(T,p)$, consistent with Eqs. (1) and (2) provided $T>0.25$ $E_g$. This $T$-independent loss of QP spectral weight $\sim\Delta\chi T(p)/\mu_B^2$ within the Fermi window illustrates two important features of the pseudogap. Firstly it shows the "non-states-conserving" property of the approximately V-shaped pseudogap in which states lost within the gap region are removed to very much higher energies. Secondly it shows that the pseudogap does not close at the characteristic pseudogap temperature $T^*$ (or indeed up to 400 K), as is widely believed. For the lowest values of $p$ the $\Delta\chi T$ curves have a negative slope at low $T$, as expected from Eq. (2) when $T<0.25E_g$. At higher $T$ the weaker negative slope probably arises from a weak decrease in $\chi_{spin}$ with tempera-

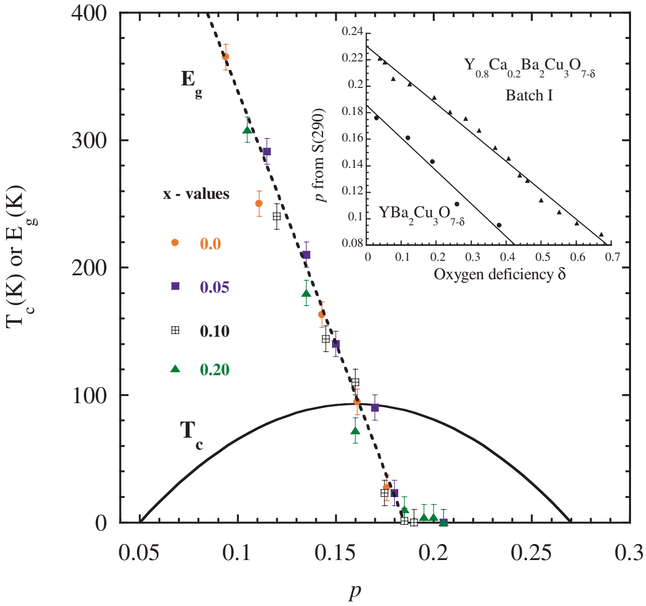


FIG. 6. (Color online) $E_g(p)$ for $Y_{1-x}Ca_xBa_2Cu_3O_{7-\delta}$ compounds. The parabolic $T_c(p)$ curve for $x=0$ with $T_{c\,\max}=93$ K is also shown. The dashed line is a guide to the eye. The inset shows how the $p$-values obtained from the room-temperature TEP varied with oxygen deficiency $\delta$ (measured via weight loss) in our earlier work (Ref. 5). Many of the susceptibility samples studied here were too small to measure $\delta$.

ture for $p>0.19$ that is also seen in OD Bi:2212.[5]

Figure 5(a) shows $\Delta\chi T(p)$ for pure Y123. Here the hole content of the reference compound is 0.176 and a small PG is present at this composition (see Fig. 5). Nevertheless, $\Delta\chi T(p)$ for pure Y123 shows almost identical behavior to that shown by the Ca-substituted samples. This lends further support to our finding that changes in $C_{\rm tot}$ with $x$ are $p$ independent. We have also fitted the $\Delta\chi T(p)$ data for the Ca-substituted samples to a V-shaped PG in the DOS, using Eqs. (1) and (2). The $E_g(p)$ values obtained from these fits are also shown in Fig. 6. In order to relate the present data to those in Ref. 5 we show plots of $p$ from the thermoelectric power (TEP) vs oxygen deficiency $\delta$ obtained from weight changes in the inset to Fig. 6. As found previously,[5,10,13,23,24] $E_g(p)$ is insensitive to the Ca content within the experimental error bars. It can be seen that $E_g(p)$ falls almost linearly with increasing hole concentration, becomes less than $T_c(p)$ on the lightly overdoped side, and vanishes for $p>0.19$.

### B. Heat-capacity data

Heat-capacity ($C_v$) data for an OD sample, Ca20 III, with a somewhat larger Curie-Weiss contribution to $\chi(T)$ than Ca20 I, are shown in Figs. 7 and 8. They were obtained using a differential technique against a pure copper reference sample. Figure 7 shows the electronic specific-heat coefficient $\gamma(H,T)=C_v/T$ of the sample in magnetic fields from 0–13 Tesla after correcting for the difference in phonon terms of the sample and the reference. The influence of magnetic fields ($H$) up to 13 Tesla is demonstrated in Fig. 8 by showing difference plots of $\Delta\gamma(H)[\equiv\gamma(H,T)-\gamma(H=0,T)]$

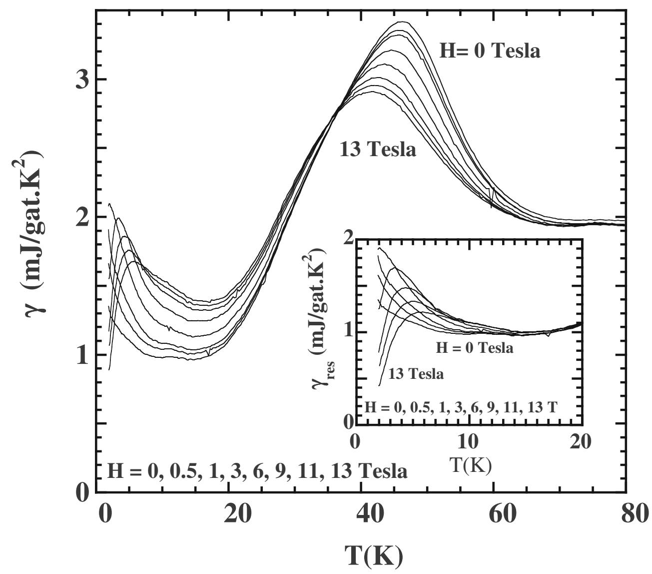


FIG. 7. Main—magnetic field and temperature dependence of the electronic specific-heat coefficient, $\gamma(H,T)$ for a third-batch of OD $Y_{0.80}Ca_{0.20}Ba_2Cu_3O_{7-\delta}$. Inset—the residual specific-heat coefficient, $\gamma_{\rm res}(H,T)$ after subtracting the contribution from superconductivity.

versus $T$. Over most of the temperature region these difference curves can be scaled to lie on the same curve by dividing them by $H\ln(90/H)$, as shown in the inset to Fig. 8. This behavior is predicted by calculations based on the theory of Bardeen, Cooper, and Schrieffer[25,26] for a $d$-wave superconductor in the dirty limit. It is also given by standard analysis of the vortex lattice in the London limit at intermediate fields, being related by thermodynamics to the $-\ln H$ term in the reversible magnetization.[27] However it is surprising that the $H\ln H$ scaling still appears to hold above $T_c$, in the range

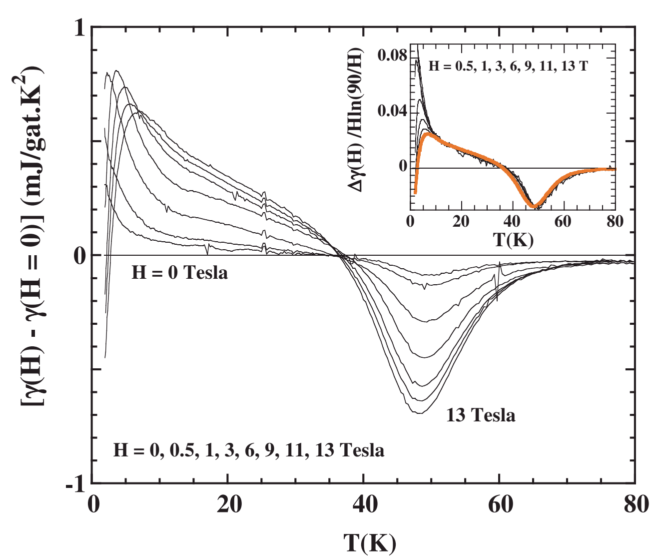


FIG. 8. (Color online) Main—difference in specific-heat coefficients $[\gamma(H,T)-\gamma(H=0,T)]$ versus $T$ for the third-batch of OD $Y_{0.80}Ca_{0.20}Ba_2Cu_3O_{7-\delta}$. Inset—scaling of the difference plot used to determine the contribution from superconductivity. The thick line represents the data at 13 Tesla.

50–65 K. Because the scaled curves can be extrapolated to zero according to an $A-BT^2$ law and have an entropy-conserving property between 70 K (well above $T_c$) and $T \rightarrow 0$, we can use them to determine the contribution, $\gamma_{sc}(H)$, from superconductivity. After subtracting $\gamma_{sc}(H,T)$ from the total electronic term $\gamma(H,T)$ we obtain the residual electronic and magnetic contributions $\gamma_{res}(H,T)$ not associated with the superconducting condensate that are shown in the inset to Fig. 7. The 13 Tesla data for $\gamma_{res}(H,T)$ extrapolate to a rather low value at $T=0$ K. This places an upper limit to any electronic contribution due to pair breaking of $\gamma(0) \sim 0.3$ mJ/gat K$^2$ at $T=0$ K. The major part of $\gamma_{res}(H,T)$ below 15 K is therefore of magnetic origin.

The low-temperature specific heat is very sensitive to the presence of paramagnetic impurities, and we now discuss the information on impurities that can be deduced from the data shown in Fig. 7. The zero-field $T$ dependences of the more important impurity phases in cuprate superconductors are summarized in a review by Junod[28] although these do not include possible impurities containing Ca. Many of these phases exhibit a magnetic transition below 20 K (usually antiferromagnetic), and the temperature and field dependences of the anomaly then provide a clear signature of the presence of the impurity phase and its concentration. Where no such anomaly is detectable in our data we estimate an upper limit for the impurity concentration assuming a resolution of $\sim 0.02$ mJ/gat K$^2$ in our data for Ca20 III. [Note that 1 gat$\equiv$1/13 mol of Y(Ca)123.] For impurity phases that do not have a magnetic transition below 20 K we compare our data with the known temperature and field dependence of the impurity phase specific heat.

The inset to Fig. 7 reveals a Schottky-like anomaly associated with very weakly interacting paramagnetic impurities, moving to higher temperatures with increasing magnetic field. We see no sign of a magnetic transition below 20 K. Green phase ($Y_2BaCuO_5$) impurity exhibits a sharp and strongly $H$-dependent specific-heat anomaly at $\sim$17–19 K due to the antiferromagnetic transition.[29] The absence of such an anomaly in the present data places an upper limit of $\sim$0.7% moles/mole Y(Ca)123 for this impurity phase. Similar arguments apply to $Y_2Cu_2O_5$ (blue phase), $Ba_2Cu_3O_5$,[30] and oxygen-deficient $BaCuO_{2+z}$, each of which exhibits a sharp and field-dependent magnetic ordering anomaly below 12 K. We discount the latter on the basis of our own $C_v$ measurements of $BaCuO_{2+z}$ after the same oxygen treatment used for Ca20 III. If the other three impurities were all present at half of our detection limit, they would contribute 26 $1\times10^{-4}$ emu K/mole to $C_{tot}$, so for Ca20 III we have included an additional impurity term of $26\pm26$ $1\times10^{-4}$ emu K/mole in Table I. Fully oxygenated $BaCuO_{2+z}$ does not undergo long-range magnetic order above 1 K, but has an unusual and distinctive field dependence because of its complex magnetic structure.[31,32] The specific heat in zero field has an unusually large low-temperature upturn, and at 2 K the specific heat decreases monotonically with increasing magnetic field. This is seen in all published data[31,32] and we have confirmed it in our own measurements on a fully oxygenated $BaCuO_{2+z}$ sample. This contrasts sharply with the behavior we observe for Ca20 III, which shows a rather weak upturn in zero-field and a field dependence at 2 K, which first increases then decreases as the Schottky anomaly moves to higher temperatures with increasing field. Detailed analysis shows that the temperature and field dependences can be fitted by a Schottky anomaly arising from 0.011 moles of (unidentified) $s=1/2$ impurities per mole Y123, plus a contribution corresponding to a maximum of 0.024 mole $BaCuO_{2+z}$ per mole Y123. The combined contribution to $C_{tot}$ from these two paramagnetic impurity phases is 131 $\times10^{-4}$ emu K/mole Y123, a factor of 4 less than the value for Ca20 III in Table I. Furthermore magnetic impurities cannot account for the rather large, temperature-independent zero-field contribution to $\gamma_{res}$. We therefore conclude that $\gamma_{res}(H,T)$ results mainly from a magnetic contribution from the Ca ions, supporting our findings from the analysis of $\chi(T)$ data. The weak-field dependence that we observe suggests a rather high-energy scale of $\sim$34 K for these excitations, which may arise from magnetic interactions or from the Kondo effect.

## IV. DISCUSSION

Bearing in mind that 1% $s=1/2$ spins per mole give a $HT$ Curie constant of 37.5 $1\times10^{-4}$ emu K/mole, the values of $C_{tot}$ shown in Table I for batches I to III of 20% Ca-Y123 correspond to 10–13% $s=1/2$ spins per mole Y123. This is much larger than estimates of impurity spin concentrations from ESR (1 and 2% for batches I and II), XRD ($\leq$1% for all samples), and $C_v$ (3.5% for batch III). So therefore the increase in $\chi(T)T$ of $Y_{1-x}Ca_xBa_2Cu_3O_{7-\delta}$ with $x$ in Figs. 1, 2, and 4 is much too large to be caused by magnetic impurities. If we subtract the impurity spin contributions and apply the usual formula $C_{corr}=xN_{av}p_{eff}^2\mu_B^2/3k_B$, where $N_{av}$ is Avogadro's number and $\mu_B$ the Bohr magneton, to the data in Table I or to the intercepts in Fig. 4, then the effective moment per $Ca^{++}$ ion is $p_{eff}=1.26\pm0.05$ (in units of $\mu_B$) irrespective of $p$. The origin of this Ca-induced magnetic moment is not entirely clear. As stated earlier, we think it is unlikely that this is related to the proposed appearance of in-plane oxygen vacancies with magnetic character.[19] In-plane disorder capable of giving such a large Curie term in the magnetic susceptibility should reduce $T_{cmax}$ more drastically. For example 20%Ca substitution only reduces $T_{cmax}$ of pure Y123 by $\sim$9 K, equivalent to $\sim$1% Zn substitution in the $CuO_2$ plane.

As shown in Fig. 9, $C_{corr}(x)$ is only approximately linear in $x$. Therefore, we examine two possible scenarios: (i) All $Ca^{2+}$ give a smaller effect with $p_{eff}\sim1.26$ (less than $p_{eff}\sim1.7$ for spin $s=\frac{1}{2}$). In this case $C_{corr}(x)$ would be linear in $x$. Furthermore, it is hard to reconcile the presence of localized spins induced by Ca, presumably in the $CuO_2$ planes, with the mobile carriers that Ca definitely induces in the $CuO_2$ planes.[10,11,33] This puzzle can be resolved by scenario (ii). An isolated $Ca^{2+}$ does not localize carriers in its vicinity, gives no magnetic moment, and donates one extra mobile carrier to the $CuO_2$ planes, but statistical clusters of two or more nearest-neighbor $Ca^{2+}$ ions cause a stronger perturbation in the neighboring $CuO_2$ planes and give rise to a magnetic moment. For $x=0.20$, the concentration of isolated $Ca^{2+}$ ion is given by $x(1-x)^4=0.082$ and that for nonisolated $Ca^{2+}$ is

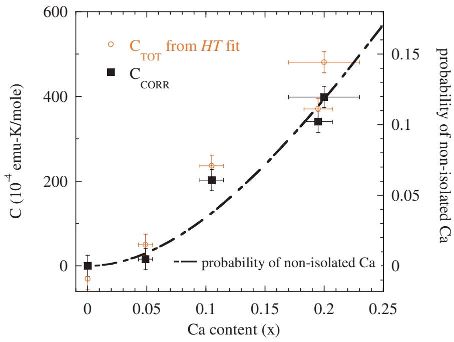


FIG. 9. (Color online) $C_{tot}$, $C_{corr}$ from Table I and the probability of nonisolated Ca atoms (dashed line) versus Ca content ($x$) determined by EPMA, for $Y_{1-x}Ca_xBa_2Cu_3O_{7-\delta}$.

$x[1-(1-x)^4]=0.118$. In this model the data in Fig. 9 give $p_{\mathrm{eff}}\sim 1.6$, closer to the value expected for $s=\frac{1}{2}$. Scenario (ii) is further supported by the following points. (i) As Fig. 9 shows, the Ca-induced Curie constant and the probability of finding nonisolated $Ca^{2+}$ have similar $x$ dependences. (ii) As shown in Fig. 10, $T_{\mathrm{cmax}}$ vs $x$ has a negative curvature, suggesting increased scattering from additional perturbations in the $CuO_2$ planes. This negative curvature contrasts with the linear $x$ dependence that would be expected in scenario (i) but would be consistent with anomalously strong scattering from Ca pairs or clusters, as in scenario (ii). (iii) This "pair" picture is also consistent with experimental evidence that Ca is less effective as a hole donor for larger $x$. For example, for nearly fully oxygenated compounds, the maximum planar hole contents are 0.203, 0.217, and 0.236 ($\pm 0.004$) for $x=0.05$, 0.1, and 0.2, respectively.[10] Whereas from simple electron counting $Ca^{2+}$ is expected to add $x/2$ holes per $CuO_2$ plane, giving 0.205, 0.23, and 0.28 for the corresponding $x$ values. A sketch showing how adjacent Ca ions give a stronger attractive potential for holes on neighboring $CuO_2$ planes is given in the inset to Fig. 10. It should be mentioned that a similar model was proposed by Hammel *et al.*[34] on the basis of their NMR measurements, when considering possible hole localization in $La_2CuO_{4+y}$ and $La_{2-x}Sr_xCuO_4$.

## V. CONCLUSIONS

In conclusion, we have reported a systematic study of the static magnetic susceptibility for polycrystalline $Y_{1-x}Ca_xBa_2Cu_3O_{7-\delta}$. From the analysis of $\chi(T)$ data we see that the pseudogap vanishes abruptly for $p>0.19$. This complements our earlier analysis of resistivity, $\rho(T,p)$, data quite well.[13,23,35,36] As $p$ is reduced below 0.19, $\chi(T)T$ decreases, and therefore the PG energy $E_g$ must increase. Within models involving preformed pairs,[2] and others in which the PG sets in abruptly below a certain temperature $T^*$, one would expect $\chi(T)T$ vs $T$ plots for samples with a PG to merge with each other at higher temperatures where the pseudogap is zero. We have not seen any sign of a recovery in $\chi(T)T$ up to 400 K (the upper temperature limit of the measurements). This implies that the pseudogap causes a permanent loss of states near the Fermi level and that it does not close as the temperature rises. The same conclusions were reached from earlier specific-heat measurements.[3–5] This places severe constraints on possible theories of the PG.

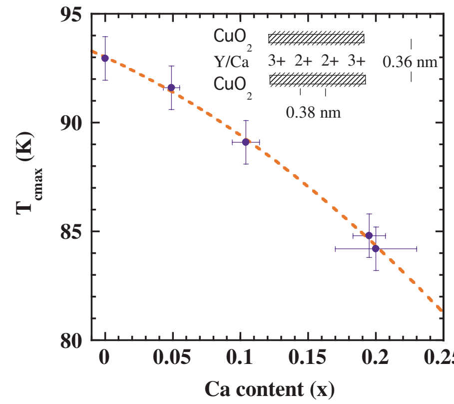


FIG. 10. (Color online) The maximum $T_c(\equiv T_{c\,\mathrm{max}})$ versus Ca content ($x$) in $Y_{1-x}Ca_xBa_2Cu_3O_{7-\delta}$. The dashed line is a guide to the eye. The inset shows a sketch of how two adjacent Ca ions give a larger attractive potential for positive holes (less attraction for electrons) on the neighboring $CuO_2$ planes.

We have also found a Curie-like contribution due to Ca substitution that is almost independent of $p$ and oxygen content and put forward a model where this arises from statistical clusters of two or more nearest-neighbor Ca atoms.

## ACKNOWLEDGMENTS

We would like to thank J. L. Tallon for preparing some of the samples and for helpful suggestions and comments on many occasions over a long period. We also thank P. Monod, K. Yates, C. Hayward, Y. Shi, and D. M. Astill for making the ESR, Raman, and EPMA measurements and C. L. Zentile for supplying a $BaCuO_2$ sample. We are grateful to P. Monod, Laboratoire de Physique du Solide (UPR 5 CNRS), Paris, France, for performing and interpreting the ESR measurements. One of us (S.H.N.) acknowledges financial support from the Commonwealth Scholarship Commission (UK), Darwin College, the Cambridge Philosophical Society, the Lundgren Fund, the Department of Physics, and the IRC in Superconductivity, Cambridge. S.H.N. also thanks the Quantum Matter group, University of Cambridge for their hospitality.

*Corresponding author. salehnaqib@yahoo.com

[1] J. W. Loram, K. A. Mirza, J. R. Cooper, W. Y. Liang, and J. M. Wade, J. Supercond. **7**, 243 (1994).
[2] T. Timusk and B. Statt, Rep. Prog. Phys. **62**, 61 (1999) and references therein.
[3] J. R. Cooper and J. W. Loram, J. Phys. IV **10**, PR3–213 (2000).
[4] J. L. Tallon and J. W. Loram, Physica C **349**, 53 (2001).
[5] J. W. Loram, J. Luo, J. R. Cooper, W. Y. Liang, and J. L. Tallon, J. Phys. Chem. Solids **62**, 59 (2001); J. W. Loram, K. A. Mirza, and J. R. Cooper, *IRC in Superconductivity - Research Review* (University of Cambridge, Cambridge, 1998), p.77.
[6] J. R. Cooper and J. W. Loram, J. Phys. IV **6**, 2237 (1996).
[7] C. Bernhard, Ch. Niedermayer, U. Binninger, A. Hofer, Ch. Wenger, J. L. Tallon, G. V. M. Williams, E. J. Ansaldo, J. I. Budnick, C. E. Stronach, D. R. Noakes, and M. A. Blankson-Mills, Phys. Rev. B **52**, 10488 (1995).
[8] C. Bernhard and J. L. Tallon, Phys. Rev. B **54**, 10201 (1996).
[9] G. V. M. Williams, J. L. Tallon, and J. W. Loram, Phys. Rev. B **58**, 15053 (1998).
[10] S. H. Naqib, Ph.D. thesis, University of Cambridge, 2003.
[11] J. L. Tallon, C. Bernhard, H. Shaked, R. L. Hitterman, and J. D. Jorgensen, Phys. Rev. B **51**, 12911 (1995).
[12] S. D. Obertelli, J. R. Cooper, and J. L. Tallon, Phys. Rev. B **46**, 14928 (1992).
[13] S. H. Naqib, J. R. Cooper, J. L. Tallon, and C. Panagopoulos, Physica C **387**, 365 (2003).
[14] M. R. Presland, J. L. Tallon, R. G. Buckley, R. S. Liu, and N. E. Flower, Physica C **176**, 95 (1991).
[15] A. Sacuto, J. Cayssol, D. Colson, and P. Monod, Phys. Rev. B **61**, 7122 (2000).
[16] N. Guskos, V. Likodimos, C. A. Londos, V. Psycharis, C. Mitros, A. Koufoudakis, H. Gamari-Seale, W. Windsch, and H. Metz, J. Solid State Chem. **119**, 50 (1995).
[17] R. Troc, J. Janicki, A. Zygmunt, H. Drulis, and A. Niedzwiedz, Physica B **193**, 1 (1994).
[18] R. Jones, R. Janes, R. Armstrong, N. C. Pyper, P. P. Edwards, D. J. Keeble, and M. R. Harrison, J. Chem. Soc., Faraday Trans. **86**, 675 (1990).
[19] V. P. S. Awana and A. V. Narlikar, Phys. Rev. B **49**, 6353 (1994).
[20] F. Rullier-Albenque, H. Alloul, and R. Tourbot, Phys. Rev. Lett. **87**, 157001 (2001).
[21] J. L. Tallon, J. W. Loram, G. V. M. Williams, J. R. Cooper, I. R. Fisher, J. D. Johnson, M. P. Staines, and C. Bernhard, Phys. Status Solidi B **215**, 531 (1999).
[22] I. Kokanovic, J. R. Cooper, S. H. Naqib, R. S. Islam, and R. A. Chakalov, Phys. Rev. B **73**, 184509 (2006).
[23] S. H. Naqib, J. R. Cooper, J. L. Tallon, R. S. Islam, and R. A. Chakalov, Phys. Rev. B **71**, 054502 (2005).
[24] S. H. Naqib and J. R. Cooper, Physica C **460-462**, 750 (2007).
[25] Y. S. Barash, A. A. Svidzinskii, and V. P. Mineev, JETP Lett. **65**, 638 (1997).
[26] C. Kübert and P. J. Hirschfeld, Solid State Commun. **105**, 459 (1998).
[27] M. Tinkham, *Introduction to Superconductivity*, 2nd edition (McGraw-Hill, New York, 1996), Chap. 5.3.2.
[28] A. Junod, in *Physical Properties of High Temperature Superconductors II*, edited by D. M. Ginsberg (World Scientific, Singapore, 1990), pp. 13–120.
[29] W. Y. Liang and J. W. Loram, Physica C **404**, 230 (2004).
[30] T. Graf, A. Junod, D. Sanchez, G. Triscone, and J. Muller, Physica C **185–189**, 473 (1991).
[31] J.-Y. Genoud, A. Mirmelstein, G. Triscone, A. Junod, and J. Muller, Phys. Rev. B **52**, 12833 (1995).
[32] R. A. Fisher, D. A. Wright, J. P. Emerson, B. F. Woodfield, N. E. Phillips, Z. R. Wang, and D. C. Johnston, Phys. Rev. B **61**, 538 (2000).
[33] M. Merz, N. Nucker, P. Schweiss, S. Schuppler, C. T. Chen, V. Chakarian, J. Freeland, Y. U. Idzerda, M. Klaser, G. Muller-Vogt, and T. Wolf, Phys. Rev. Lett. **80**, 5192 (1998).
[34] P. C. Hammel, B. W. Statt, R. L. Martin, F. C. Chou, D. C. Johnston, and S.-W. Cheong, Phys. Rev. B **57**, R712 (1998).
[35] S. H. Naqib, R. A. Chakalov, and J. R. Cooper, Physica C **407**, 73 (2004).
[36] S. H. Naqib, J. R. Cooper, R. S. Islam, and J. L. Tallon, Phys. Rev. B **71**, 184510 (2005).